63-4-

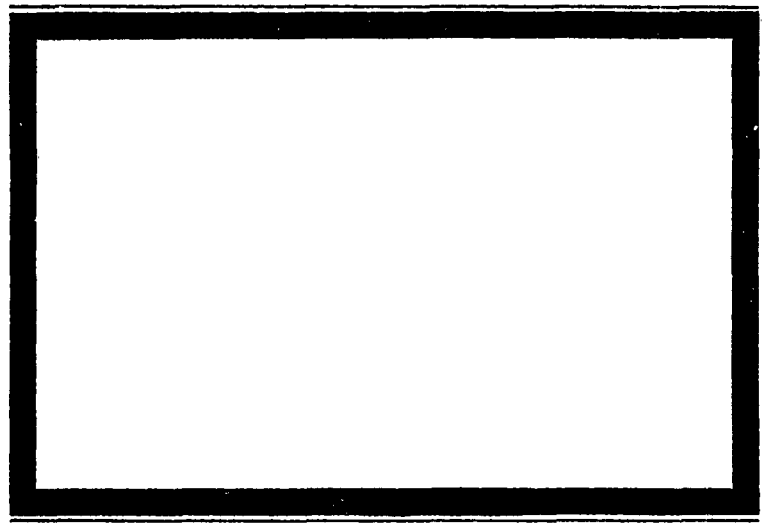

SR-18

THE MITRE CORPORATION
Middlesex Turnpike, Rte. 62 Bedford, Massachusetts

ON THE APPLICATION OF THE THEORY OF LOCKING MEDIA TO GROUND SHOCK PHENOMENA

by

Paul Weidlinger, Consulting Engineer, 400 Madison Avenue, New York 17, N. Y.

26 September 1960

2. The research reported in this document was supported by the Department of the Air Force under Air Force Contract AF-33 (600) 39852.

FORWARD

The MITRE Corporation is concerned with the survivability of the Air Force Command and Control Systems. It conducts studies in this general area in order to determine the levels at which various systems components fail and investigates various alleviating measures which may be employed to raise the levels of survivability.

One phase of this work is concerned with the behavior of deep underground hard command posts excavated in soil and rock when subjected to nuclear attack.

This document reports on some of the work being done by Paul Weidlinger, Consulting Engineer, New York City.

John J. O'Sullivan
The MITRE Corporation

Table of Contents

SYNOPSIS

Recent investigations on groundshock phenomena indicate that the dynamic response of certain non-linear (locking) media, may approximate the behavior of cohesive granular soils and porous rock under high pressures. There is a considerable body of fairly recent American and USSR scientific literature on this topic. It seems that the Russian investigations parallel our efforts in this field. The theory of wave propagation in such materials should have application to the design of underground shelters at very high pressure levels and may shed some additional light, by these relatively simple means on problems associated with phenomena near ground zero, in case of surface bursts or underground explosions. In Sections II and III results of current investigations are presented.

I. RECENT AND CURRENT INVESTIGATIONS.

As a result of our investigations into groundshock phenomena in the recent years, we have conjectured that the behavior of porous or granular solids (such as dry sand or porous rock) could be characterized by a medium which under uniaxial compression exhibits a stress-strain diagram which tends to become parallel with the stress axis beyond a certain critical strain, (Figure 1). Such a stress-strain diagram may be replaced by various bi-linear approximations, and such materials are currently referred to as locking media, or materials of limited compressibility, (Figure 2a, b, c, d).

The static behavior of such materials has been explored to a considerable extent since about 1957 [References 1, 2, 3, 4].

The dynamic problem for the case of the upwards curving stress-strain diagram has been considered previously, [References 5 and 6], but the assumption of a stress-strain curve having a continuous derivative, (Figure 1) makes it difficult to obtain closed form solutions. Some more recent efforts in this direction provide additional results for specific initial conditions, [Reference 7].

The linear approximations shown on Figure 2a, b, c have resulted in relatively simple solutions and some of these results have been applied with some success to the prediction of groundshock phenomena, [References 8 and 9] and have also been published in the open literature, [References 10 and 11]. A medium which shows a residual elasticity, (Figure 2d), is treated in Section II of this report.

If the two or three dimensional case is considered, one may replace the stress-strain diagram of the uniaxial case with a stress-dilatation diagram to obtain similar results. After the critical value of the dilatation is reached, a post compaction yield condition must be specified. One may, for example, assume that the medium behaves like an inviscid fluid or that it follows Coulombs law of failure. Such a medium for the case of spherical symmetry is treated in Section III of this report.

During our researches into this subject we also noted that a considerable interest in these topics exists in the USSR, as shown by Reference 12, 13, 14, 15, 16 and 17. It appears, that the Russian investigations parallel our own efforts, and the extensive numerical work of Reference 17, indicates that the application of these researches is probably also seriously considered. Significantly, most of these papers are directed towards problems associated with explosions and apparently the USSR researchers suffer from lack of experimental data just as much as our own investigations do.

As the result of our own work and the review of the USSR literature, it is believed that these investigations have application to the following topics of current interest:

(a) Groundshock phenomena in dry granular and cohesive soils, and porous rock.

(b) Feasibility studies for the design of underground shelters near ground zero.

(c) Groundshock phenomena in the neighborhood of ground zero of surface bursts.

(d) Phenomena associated with nuclear explosions contained in underground cavities.

Numerical evaluations in a few specific cases leads us to believe that this approach may indeed contribute to the solution of the above problem, [References 18 and 19]. It appears that the intrinsic dissipative behavior of the medium is the crucial characteristic which makes it appropriate for such investigations. Further theoretical and experimental work in this field may be quite fruitful.

In the following Sections II and III of this report some additional contributions to the theory of locking media are presented.

In Section II a medium with a stress-strain diagram as shown on Figure 2d is considered. The purpose of this investigation is to clarify the effects of "residual elasticity", that is, elastic action which persists after compaction or locking has occurred. This modification of the stress-strain relationship is of importance since it brings the idealized theory closer to the anticipated behavior of real materials. In our first and second report to the MITRE Corporation [References 18 and 19] the effects of this behavior were numerically evaluated, and it was shown that small residual elasticity after compaction does not significantly influence the attenuation of peak stresses in the medium at depth of 500 feet or more, as compared to a locking medium without such residual elasticity. This medium also permits us to draw certain conclusions regarding non-linear effects due to the influence of the high intensity airslap in the vicinity of ground zero.

In Section III spherical waves in an ideal locking medium are investigated. These results prove to be useful in clarifying the close-in effects of the exploding casing at the point of impact. Numerical evaluations of this work will appear in our subsequent reports on this subject.

REFERENCES - BIBLIOGRAPHY TO SECTION I

1. "On Ideal Locking Materials" by W. Prager, Transactions of the Society of Rheology, Vol. I, 1957, pp 169-175.

2. "Elastic Solids of Limited Incompressibility" by W. Prager, Proceedings of the IX Int. Congress of Applied Mechanics, Brussels 1957.

3. "A Theory of Ideal Locking Materials" by Aris Phillips, Yale University, February 1958, NR-064-415.

4. "The Thick-Walled Hollow Sphere of An Elastic-Locking Material" by Aris Phillips and Asim Yildz, Yale University, December 1959, NR-064-415.

5. "Propagation of Plastic Deformation in Solids" by Theodore Von Karman and P. E. Dawef Proceedings VI Int. Congress of Applied Mechanics 1946.

6. "The Propagation of Plasticity in Uniaxial Compression" by M. P. White and L. Griffin, Journal of Applied Mechanics, Vol. 15, 1948, p 256.

7. "Propagation of Plane Waves in Gramular Materials, Part I." by S. Katz and T. J. Ahronsy, Ballistic Research Laboratory.

8. "Induced Ground Shock in Gramular Media", Report No. 1 by Mario G. Salvadori and Paul Weidlinger, Space Technology Laboratory, Ballistic Missile Division, March 1958.

9. "Induced Ground Shock in Granular Media", Report No. 2 by Mario G. Salvadori and Paul Weidlinger, Space Technology Laboratory, Ballistic Missile Division, July 1958.

10. "Stress Waves in Dissipative Media" by Mario G. Salvadori, Richard Skalak and Paul Weidlinger, Transactions The New York Academy of Sciences Ser. II, Volume 21, No. 5, Pp 427-434, March 1959.

11. "Waves and Shocks in Locking and Dissipative Media" by Mario G. Salvadori, Richard Skalak and Paul Weidlinger, Journal of Engineering Mechanics Division ASCE, April 1960.

12. "On the Dynamics of Ground Masses" by Ishlinskii, A.I.W., and N. V. Stepananbo, DAN 1954, t. 95, No. 5.

13. "On the Plane Motion of Sand" by Ishlinskii, A.I.W., Ukr. Mathematical Journal, 1954, t. 6, No. 4.

14. "Shock Waves in a Plastic Compressible Medium" by Kompaneets, A. S. DAN 1956, t. 109, No. 1.

15. "On the General Equations of the Dynamics of Solids" by Grigorian S.S., DAN, 1959, t. 124, No. 2.

16. "On the Emission of An Elastic Wave From a Spherical Explosion in the Ground" by N. V. Zvolinskii, PMM, Vol. 24 No. 1, 1960 pp 126-133.

17. "Similarity Relations During An Explosion in a Plastic-Compacting Medium" by E. E. Lovetskii, I.A.N. 1958, No. 1 pp 120-122.

18. "Progress Report on Ground Shock at High Intensity Pressure Levels" by Paul Weidlinger, (Secret), The MITRE Corporation, October 1959.

19. "Vulnerability of Underground Installations-Second Progress Report on Ground Shock Phenomena" by Paul Weidlinger, (Secret), The MITRE Corporation, March 1960.

FIG. 1

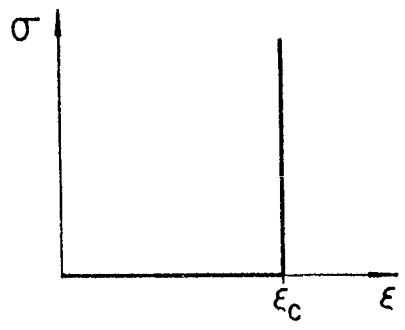

(a)

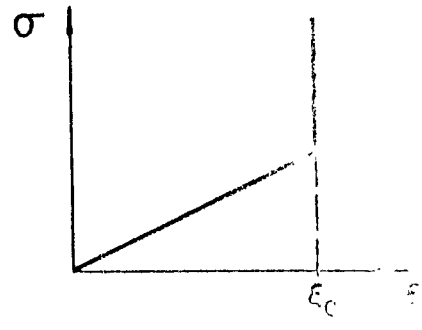

(b)

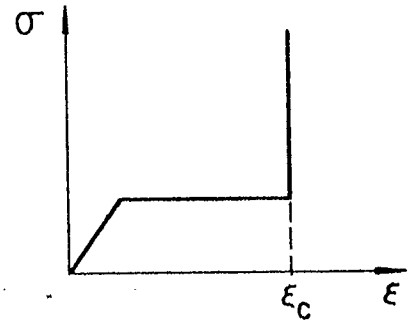

(c)

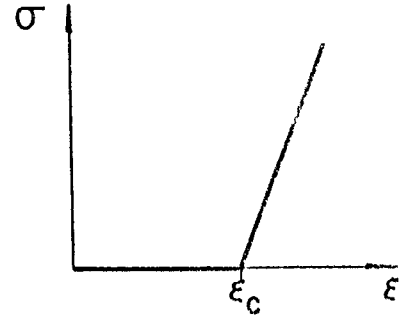

(d)

FIG. 2

SECTION II

WAVE PROPAGATION IN A PLASTIC-ELASTIC MEDIUM

By

Richard Skalak

I. STATEMENT OF PROBLEM.

The response of a semi-infinite body of plastic-elastic medium, Figure 1, is to be found due to a blast wave pressure applied to the surface of the medium. The stress-strain curve of the material is shown in Figure 2. The pressure loading is assumed to be applied to the entire surface of the medium so that the problem is one-dimensional. The type of time history of the surface pressure considered is shown in Figure 3. The strains are assumed to be small throughout.

II. GOVERNING EQUATIONS.

(a) The Shock Wave.

The applied loading generates a plane shock wave which compresses the medium from its initial state to a state corresponding to some point on the inclined portion of the stress-strain curve. The velocity of propagation of this shock wave at any time is

$$\dot{z}_s = \sqrt{\frac{\bar{E}}{\rho}} \tag{1}$$

where $\bar{E}$ is the secant modulus of elasticity, Figure 2

$$\bar{E} = \sqrt{\frac{\sigma_{zs}}{\epsilon_s}} \tag{2}$$

where σ_{zs}, ϵ_s are the normal vertical stress and strain immediately behind the shock front, the density ρ is assumed constant because the strains are assumed to be small.

The particle velocity behind the shock wave is

$$\dot{u}_s = \frac{\sigma_{zs}}{\rho \dot{z}_s} \tag{3}$$

In terms of the modulus E of the inclined portion of the stress-strain curve, Figure 2, the value of ϵ_s can be written as

$$\epsilon_s = \epsilon_c + \frac{\sigma_{zs}}{E} = \epsilon_c + \frac{\sigma_{zs}}{\rho c^2} \tag{4}$$

where ϵ_c is the plastic strain shown in Figure 2, and $c^2 = E/\rho$.

From Equations (1) through (4) it follows that:

$$\sigma_{zs} = \rho \epsilon_c \dot{z}_s^2 \frac{1}{1 - (\frac{\dot{z}_s}{c})^2} \tag{5}$$

$$u_s = \epsilon_c \dot{z}_s \frac{1}{1 - (\frac{\dot{z}_s}{c})^2} \tag{6}$$

(b) Region Behind the Shock Wave.

Behind the shock wave the state of the medium is assumed to correspond to points on the inclined portion of the stress-strain curve, Figure 2. If u is the downward displacement of any particle from its original position, the equation of motion is:

$$\frac{\partial \sigma_z}{\partial z} = - \rho \frac{\partial \dot{u}}{\partial t} \tag{7}$$

By definition, considering compressive strains positive,

$$\epsilon = - \frac{\partial u}{\partial z} \tag{8}$$

Since ϵ_c is a constant, (8) yields

$$\frac{\partial (\epsilon - \epsilon_c)}{\partial t} = - \frac{\partial \dot{u}}{\partial z} \tag{9}$$

From Equation (9) and

$$\sigma_z = (\epsilon - \epsilon_0) E \tag{10}$$

it follows

$$\frac{1}{E}\frac{\partial \sigma_z}{\partial t} = - \frac{\partial \dot{u}}{\partial z} \tag{11}$$

The $\dot{u}$ in Equations (7) and (11) is the particle velocity. From these equations,

$$\frac{\partial^2 \sigma_z}{\partial t^2} = c^2 \frac{\partial^2 \sigma_z}{\partial z^2} \qquad \text{and}$$

$$\frac{\partial^2 \dot{u}}{\partial t^2} = c^2 \frac{\partial^2 \dot{u}}{\partial z^2} \tag{12}$$

III. SOLUTION FOR A GIVEN SURFACE PRESSURE HISTORY.

Consider a general field point (z, t) in Figure 4 and two points labeled 1 and 2 on the shock curve located by the characteristics passing through the field point as shown in Figure 4. By virtue of Equations (7), (11) and (12), the entire field behind the shock wave has the form

$$\sigma_z = f(z - ct) + g(z + ct) \tag{13}$$

$$\dot{u} = \frac{c}{E}\left[f(z - ct) - g(z + ct)\right] \tag{14}$$

where f and g are unknown functions.

Writing Equations (13) and (14) for the point 2 in Figure 4:

$$\sigma_{z2} = f(z_2 - ct_2) + g(z_2 + ct_2) \tag{15}$$

$$\dot{u}_2 = \frac{c}{E}\left[f(z_2 - ct_2) - g(z_2 + ct_2)\right] \tag{16}$$

From (15) and (16)

$$f(z_2 - ct_2) = \frac{1}{2}\sigma_{z2} + \frac{E}{2c}\dot{u}_2 \qquad (17)$$

and since along the characteristic (z - ct) is constant, it follows that for the field point z, t indicated in Figure 4

$$f(z - ct) = \frac{1}{2}\sigma_{z2} + \frac{E}{2c}\dot{u}_2 \qquad (18)$$

Similarly, considering point 1 it is found that for the field point z, t

$$g(z + ct) = \frac{1}{2}\sigma_{z1} - \frac{E}{2c}\dot{u}_1 \qquad (19)$$

The solution for any field point can now be expressed in terms of values σ_{zs} and $\dot{u}_s$ directly behind the shock front by substituting (18) and (19) into (13) and (14):

$$\sigma_z = \frac{1}{2}(\sigma_{z1} + \sigma_{z2}) - \frac{E}{2c}(\dot{u}_1 - \dot{u}_2) \qquad (20)$$

$$\dot{u} = \frac{1}{2}(\dot{u}_1 + \dot{u}_2) - \frac{c}{2E}(\sigma_{z1} - \sigma_{z2}) \qquad (21)$$

The location of the shock front $z_s(t)$ and the values of stress and velocity σ_{zs} and $\dot{u}_s$ at the shock front are unknown in advance for a given surface pressure history. However, if the location of the shock wave $z_s(t)$ is determined, then σ_{zs} and $\dot{u}_s$ are given by Equations (5) and (6) and the remainder of the field can be found from (20) and (21). The solution is completed by establishing $z_s(t)$ for a given surface pressure history as follows:

Consider a field point which is on the surface z = 0 as shown in Figure (5). For this point the stress σ_z given by Equation (20) is the applied pressure p at time t. By substituting the values for σ_{zs} and $\dot{u}_s$

from Equations (5) and (6) into Equation (20), an equation relating p, z_1, and z_2 is obtained, which after simplification reads:

$$\frac{2}{E\epsilon_c} p = \frac{\dot{z}_2}{c - \dot{z}_2} - \frac{\dot{z}_1}{c + \dot{z}_1} \tag{22}$$

If the point (0, t) in Figure (5) is assumed to move along the t axis, the pressure p(t) is the given surface pressure history. The heights shown in Figure (5) labeled z_1 and z_2 may then be also considered to be functions of t. Similarly the times t_1 and t_2 may be considered as functions of t. The time t_1 is related to t by

$$t_1 = t - \frac{z_1}{c} \tag{23}$$

Differentiating with respect to t,

$$\frac{dt_1}{dt} = 1 - \frac{1}{c} \frac{dz_1}{dt_1} \frac{dt_1}{dt} \tag{24}$$

The derivative $\frac{dz_1}{dt_1}$ is what is meant by $\dot{z}_1$ in Equation (22), for example. From Equation (24)

$$\frac{dt_1}{dt} = \frac{c}{c + \dot{z}_1} \tag{25}$$

Defining z_1' to be the derivative $\frac{dz_1}{dt}$, it follows, using Equation (25),

$$z_1' = \frac{dz_1}{dt} = \frac{dz_1}{dt_1} \frac{dt_1}{dt} = \frac{\dot{z}_1 c}{c + \dot{z}_1} \tag{26}$$

Similarly, using

$$t_2 = t + \frac{z_2}{c} \tag{27}$$

it is found that

$$z_2' = \frac{dz_2}{dt} = \frac{\dot{z}_2 c}{c - \dot{z}_2} \tag{28}$$

From Equations (26) and (28)

$$\frac{z_1'}{c} = \frac{\dot{z}_1}{c + \dot{z}_1} \quad \text{and} \quad \frac{z_2'}{c} = \frac{\dot{z}_2}{c - \dot{z}_2} \tag{29}$$

Substituting Equations (29) into (22)

$$\frac{2c}{E\epsilon_c} p = z_2' - z_1' \tag{30}$$

where p is p(t) and the primes denote differentiation with respect to this same t. Equation (30) can then be integrated with respect to t to yield the final equation

$$\frac{2c}{E\epsilon_c} I(t) = z_2 - z_1 \tag{31}$$

where I(t) is the impulse of the applied pressure per unit area defined by

$$I(t) = \int_0^t p \, dt \tag{32}$$

The boundary condition $z_2 = z_1 = 0$ at $t = 0$ was also used in deriving (31).

Equation (31) defines the locus $z_s(t)$ of the shock location in the z, t plane and completes the solution of the problem.

IV. COMPUTATIONAL PROCEDURE.

The Equation (31) may be used to solve for the location of the shock front z_2 at a time t_2 when the position z_1 is known for the earlier time t_1. To begin the computations using Equation (31) it is necessary to establish z_1 at some early time t_1 as a starting point. A first and a second approximation are given below and higher order approximations can be developed by similar procedures.

a) First Approximation for Short Times.

A pressure time history such as shown in Figure 3 could be replaced by a constant pressure p_a for a short time t_o so that the impulse during this interval is conserved. Then for the time interval selected $\dot{z}_2$ is a constant $\dot{z}_{20}$ and may be computed from Equation (5):

$$\dot{z}_{20} = c\sqrt{\frac{p_a}{\rho c + p_a}} \tag{33}$$

The value of z_2' is also a constant z_{20}' and is given by Equation (28). Then

$$\left[z_2\right]_{t=t_o} = z_{20} = z_{20}' t_o \tag{34}$$

A starting point is now established by using

$$z_1(t) = z_{20} \tag{35}$$

and

$$t = t_o + \frac{2z_{20}}{c} \tag{36}$$

b) Second Approximation for Short Times.

A pressure time history such as shown in Figure 3 can be represented by a Taylor series:

$$p(t) = p_o + p_o' t + p_o'' \frac{t^2}{2} + \cdots\cdots \tag{37}$$

The values of z_1 and z_2 may also be written in series form:

$$z_1 = k_1 t + k_2 t^2 + k_3 t^3 + \cdots\cdots \tag{38}$$

$$z_2 = m_1 t + m_2 t^2 + m_3 t^3 + \cdots\cdots \tag{39}$$

The impulse applied at the surface, Equation (32) is:

$$1(t) = p_o t + p_o' \frac{t^2}{2} + p_o'' \frac{t^3}{6} + \ldots . \qquad (40)$$

Substituting (38), (39) and (40) into Equation (30) and equating coefficients of each power of t yields:

$$\frac{2c}{E\mathfrak{a}_c} p_o = m_1 - k_1 \qquad (41)$$

$$\frac{c}{E\mathfrak{a}_c} p_o' = m_2 - k_2 \qquad (42)$$

etc. . . . .

The functions $z_1(t)$, Equation (38), must also be such that at the appropriate time it is equal to the value of z_2 of an earlier time. This requirement may be written as:

$$z_1(t) = z_2\left(t - \frac{2z_1(t)}{c}\right) \qquad (43)$$

where all brackets mean "a function of". Substituting (38) and (39) in Equation (43) yields

$$\begin{aligned} k_1 t + k_2 t^2 + k_3 t^3 + \ldots . = {} & m_1\left(t - \tfrac{2}{c}(k_1 t + k_2 t^2 + k_3 t^3 + \ldots)\right) \\ & + m_2\left(t - \tfrac{2}{c}(k_1 t + k_2 t^2 + k_3 t^3 + \ldots)\right)^2 \\ & + m_3\left(t - \tfrac{2}{c}(k_1 t + k_2 t^2 + k_3 t^3 + \ldots)\right)^3 \\ & + \text{etc}\ldots \qquad (44) \end{aligned}$$

Equating coefficients of each power of t in Equation (44), after expanding each term gives

$$k_1 = m_1\left(1 - \frac{2k_1}{c}\right) \tag{45}$$

$$k_2 = -m_1 \frac{2k_2}{c} + m_2\left(1 - \frac{2k_1}{c}\right)^2 \tag{46}$$

etc...

Equations (41) and (45) may be solved for k_1, m_1:

$$k_1 = \frac{cp_o}{E\epsilon_c}\left[-1 + \sqrt{1 + \frac{E\epsilon_c}{p_o}}\right] \tag{47}$$

$$m_1 = \frac{cp_o}{E\epsilon_c}\left[1 + \sqrt{1 + \frac{E\epsilon_c}{p_o}}\right] \tag{48}$$

Equations (42) and (46) may be solved for k_2, m_2 considering k_1, m_1 known:

$$k_2 = \frac{cp'_o}{E\epsilon_c} \frac{k_1^3}{m_1^3 - k_1^3} \tag{49}$$

$$m_2 = \frac{cp'_o}{E\epsilon_c} \frac{m_1^3}{m_1^3 - k_1^3} \tag{50}$$

Equation (39) can now be used with the coefficients m_1, m_2 given by (48) and (50) to derive the second approximation of z_2 corresponding to the approximation of the surface pressure by the first two terms of (37). If this approximation is considered adequate up to a time t_o, then the value of z_2 at this time is z_{20}:

$$z_{20} = m_1 t_o + m_2 t_o^2 \tag{51}$$

A starting point $z_1(t)$ for the computations using Equation (31) is now obtained by substituting (51) into (35) and (36).

It may be shown that using only the first term of (51) is equivalent to the first approximation given above.

It should be noted that in any case, in the successive steps using Equation (31), z_2 is computed first from Equation (31) and then t_2 is computed from Equation (27). The next step starts from $z_1(t)$ computed by Equations (35) and (36) using z_2 in place of z_{20} and t_o.

V. NUMERICAL EXAMPLE:

The following data are chosen as an illustration:

$$\epsilon_c = 0.02$$
$$E = 1 \times 10^6 \text{ psi}$$
$$\rho = 4.04 \text{ slugs/ft}^3$$

From these data

$$C = 5{,}960 \text{ ft/sec}$$

The pressure time history at the surface is assumed given as shown in Figure 6. The peak pressure p_o at $t = 0$ is not shown but was 184,000 psi. The impulse for the assumed loading is shown in Figure 7.

The computation is begun by applying the first approximation discussed above for the first 10 milliseconds. Equation (31) is then applied repeatedly to develop the z_s versus t curve shown in Figure 8. From Equation (22), $\dot{z}_s$ can be derived for various t and σ_{zs}, u_s can be computed from Equations (5) and (6). Figure 8 shows the values of z_s, σ_{zs} and $\dot{u}_s$ plotted versus t.

To find the stress and velocity at a field point $z = 500$ feet, $t = 200$ ms, the characteristics through this point are drawn to locate points

1 and 2 on the z_s versus t curve as shown in Figure 8. Reading the σ_{zs} and u_s curves directly below points 1 and 2 yields the values

$$\sigma_{z2} = 4{,}000 \text{ psi} \qquad u_2 = 58 \text{ ft/sec}$$

$$\sigma_{z1} = 10{,}000 \text{ psi} \qquad u_1 = 103 \text{ ft/sec}$$

Substituting these values into Equations (20) and (21) yields the field values for z = 500 feet, t = 200 ms:

$$\sigma_z = 3{,}230 \text{ psi} \qquad u = 62.6 \text{ ft/sec}$$

The values of σ_z and u at the surface and at depths of 500 and 700 feet were computed for various times. The results are plotted in Figures 6 and 9 against time after arrival of the shock wave for each point.

VI. COMPARISON OF PLASTIC-ELASTIC MEDIUM TO A LOCKING MEDIUM.

The blast pressure at the surface z = 0 derived in the example above for a plastic-elastic medium was applied to a locking medium also for comparison of the responses of the two media. The locking medium is defined by the stress-strain curve shown in Figure 10.

The response of a locking media to a given surface pressure of the type shown in Figure 3 has been studied in Reference [1] . . . The results may also be derived as a limiting case ($c \to \infty$) of the problem treated above. The location of the shock wave front at any time is given by

$$z_s = \left[\frac{2}{\rho \epsilon_c} \int_0^t I(t)\, dt \right]^{1/2} \qquad (52)$$

---

[1] Salvadori, Mario G.; Skalak, Richard, and Weidlinger, Paul "Stress Waves in Dissipative Media" Transactions of the New York Academy of Sciences, Ser. II, Vol. 21, No. 5, Pages 427-434.

where I(t) is the impulse applied at the surface from time zero to time t:

$$I(t) = \int_0^t p\,(t)\,dt \tag{53}$$

Figure 7 shows the impulse of the surface pressure used in the present examples. The stress immediately behind the shock front is

$$\sigma_{zs} = \frac{1}{\rho \epsilon_c} \left[\frac{I(t)}{z_s} \right]^2 \tag{54}$$

and the particle velocity for all particles behind the wave front is:

$$\dot{u} = \frac{I(t)}{\rho z_s} \tag{55}$$

The numerical results for the following assumed values are shown in Figure 11:

$$\rho = 4.04 \text{ slugs/ft}^3$$

$$\epsilon_c = 0.02$$

These are the same values as assumed for the plastic-elastic medium. The vertical stress and particle velocity immediately behind the shock wave-front in the plastic-elastic medium due to the same surface pressure are shown in Figure 11 also for comparison. In both cases the stresses shown are the peak stresses experienced at a given depth. The same is true of the particle velocities.

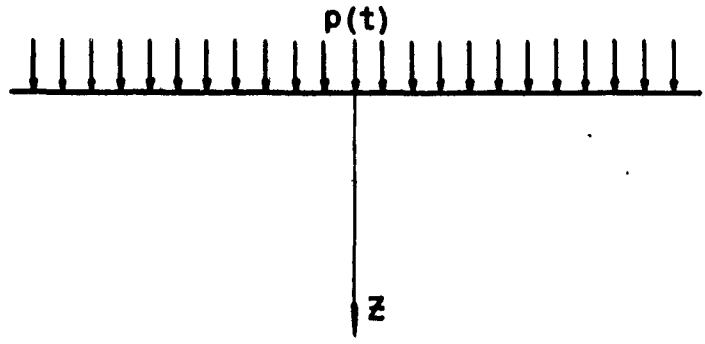

FIG. 1 SEMI – INFINITE MEDIUM

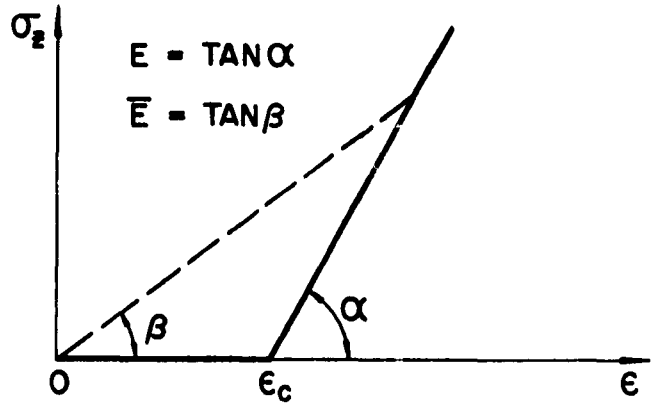

FIG. 2 STRESS – STRAIN CURVE

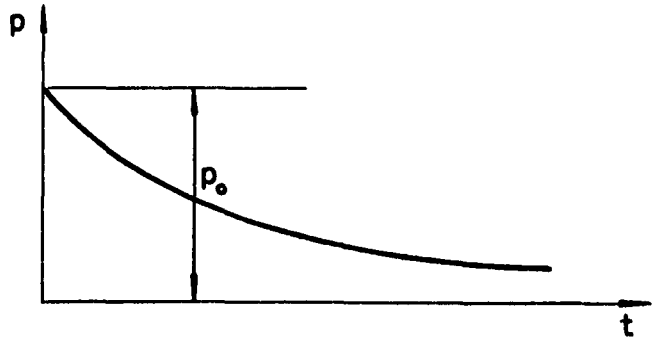

FIG. 3 SURFACE PRESSURE HISTORY

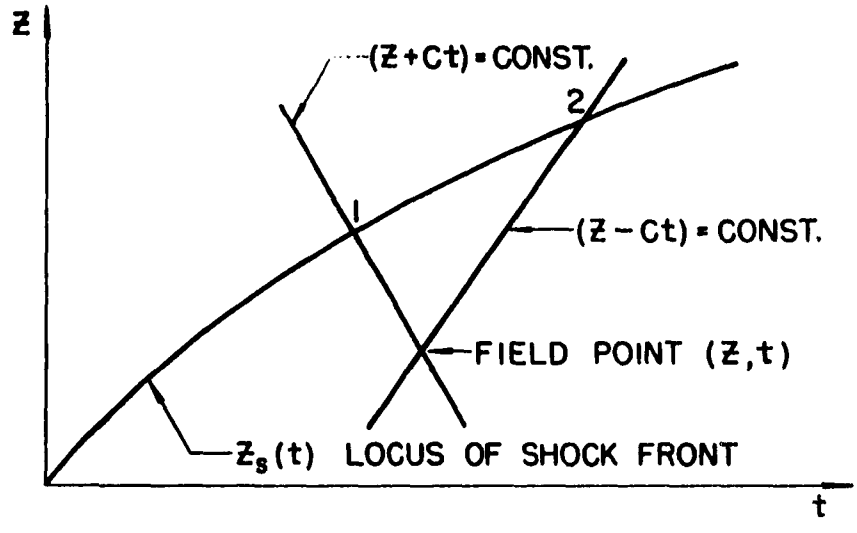

FIG. 4 SPACE — TIME PLANE

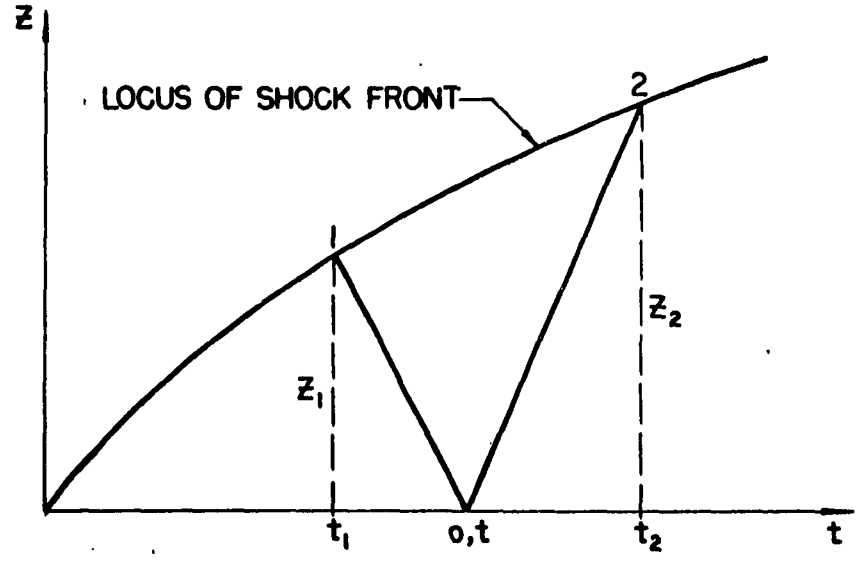

FIG. 5 FIELD POINT AT SURFACE z = 0

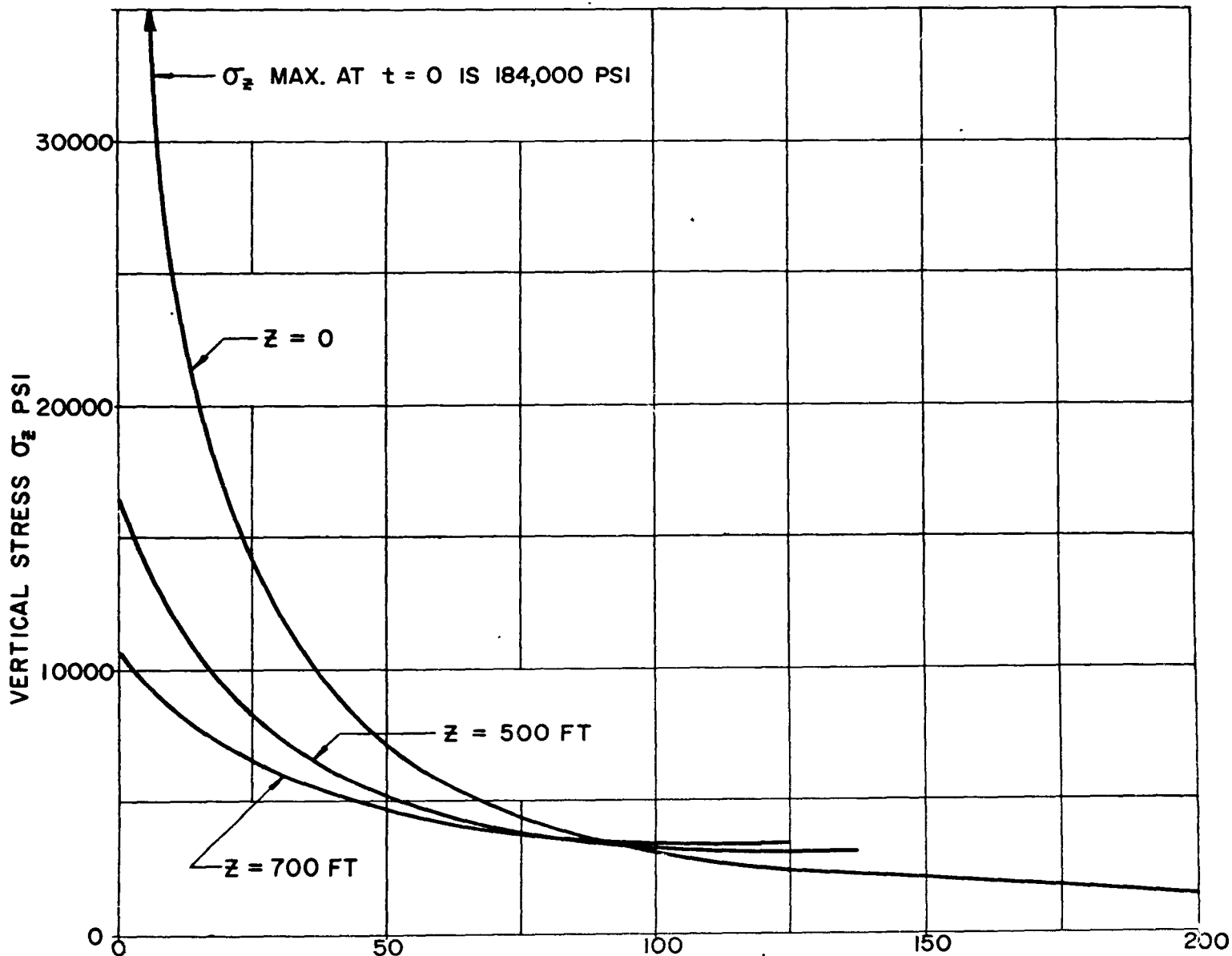

FIG. 6 STRESSES σ_z IN PLASTIC-ELASTIC MEDIUM

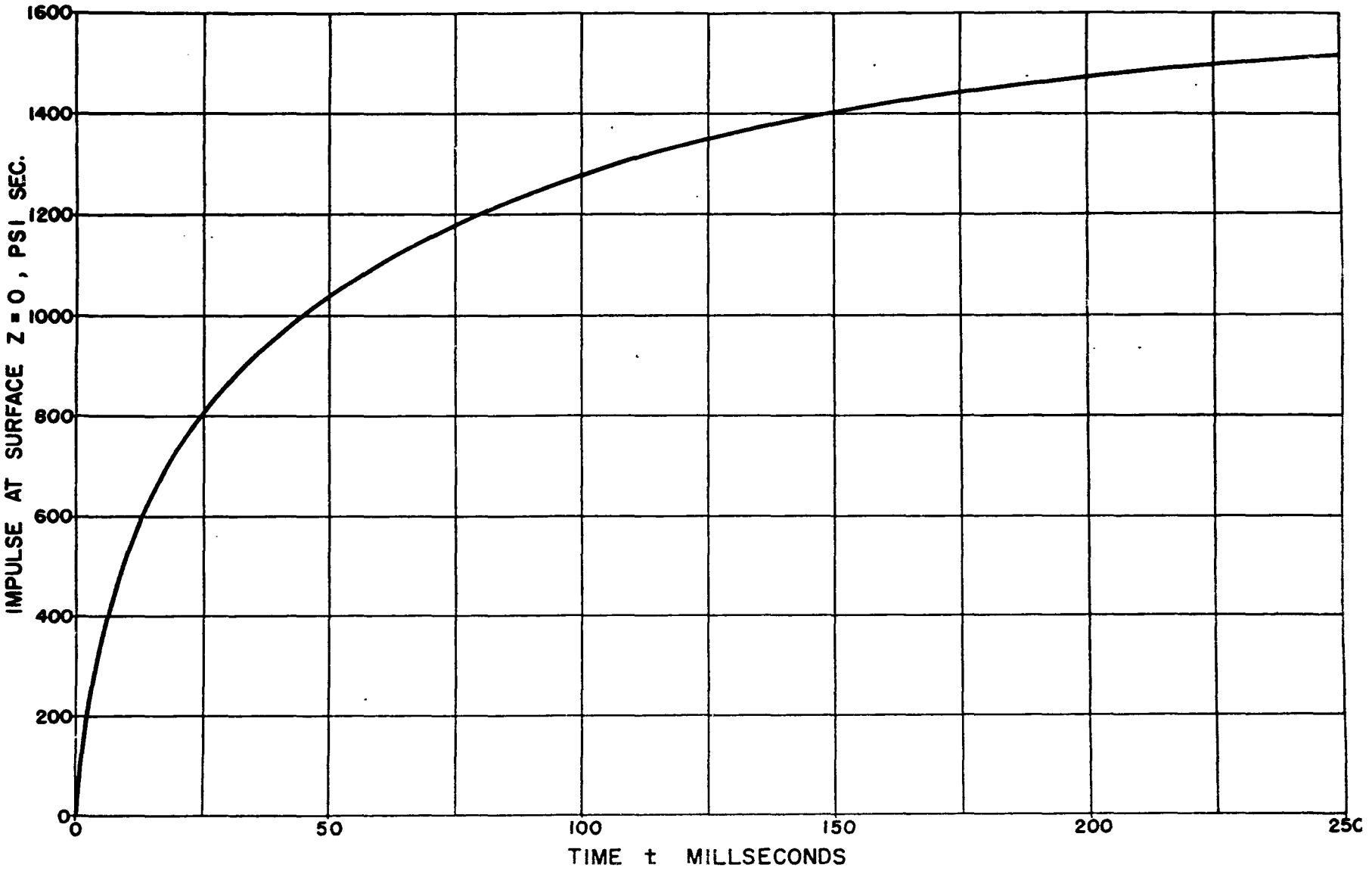

FIG. 7 IMPULSE AT SURFACE Z = 0

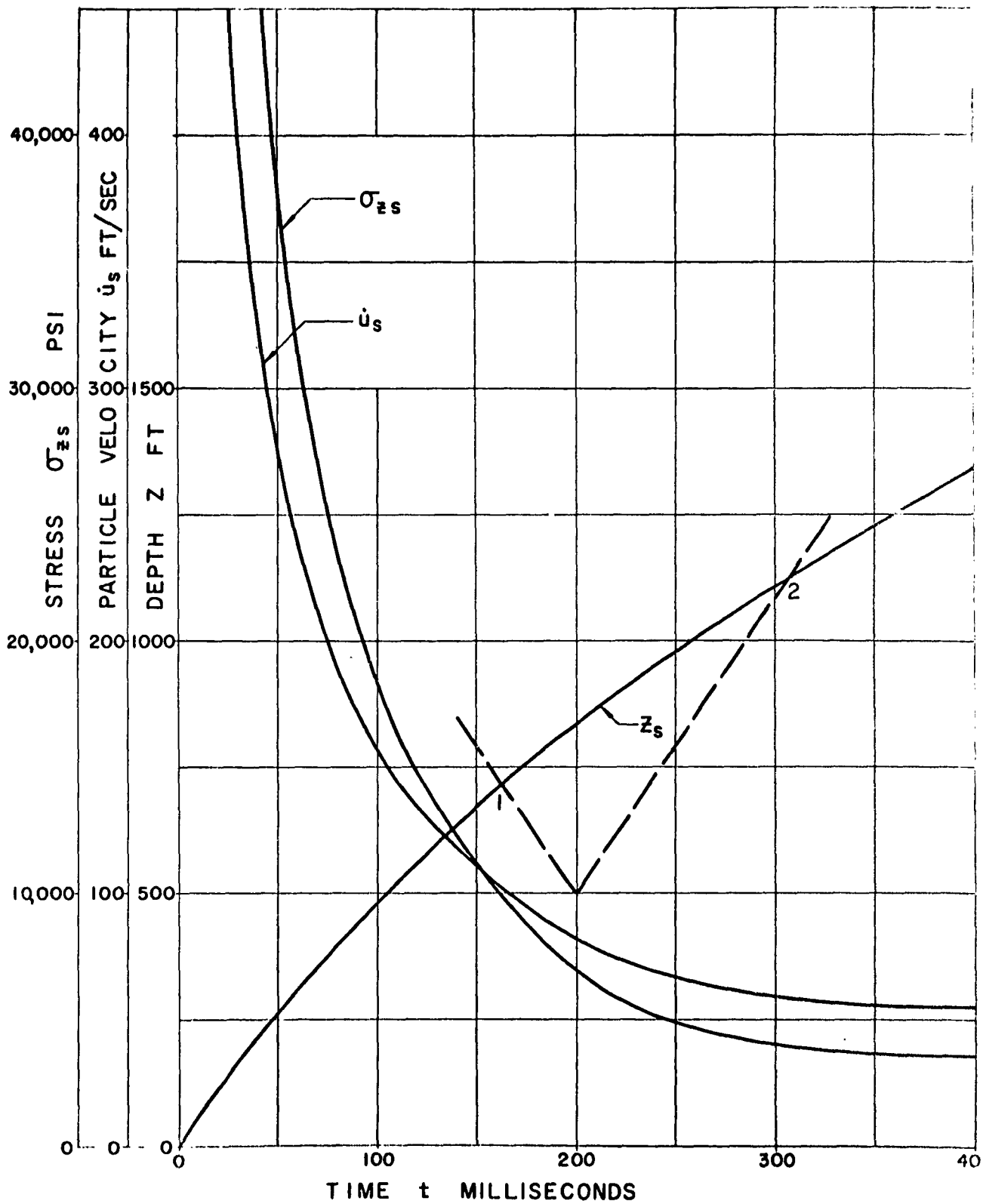

FIG 8 SPACE TIME PLOT FOR PLASTIC ELASTIC MEDIUM

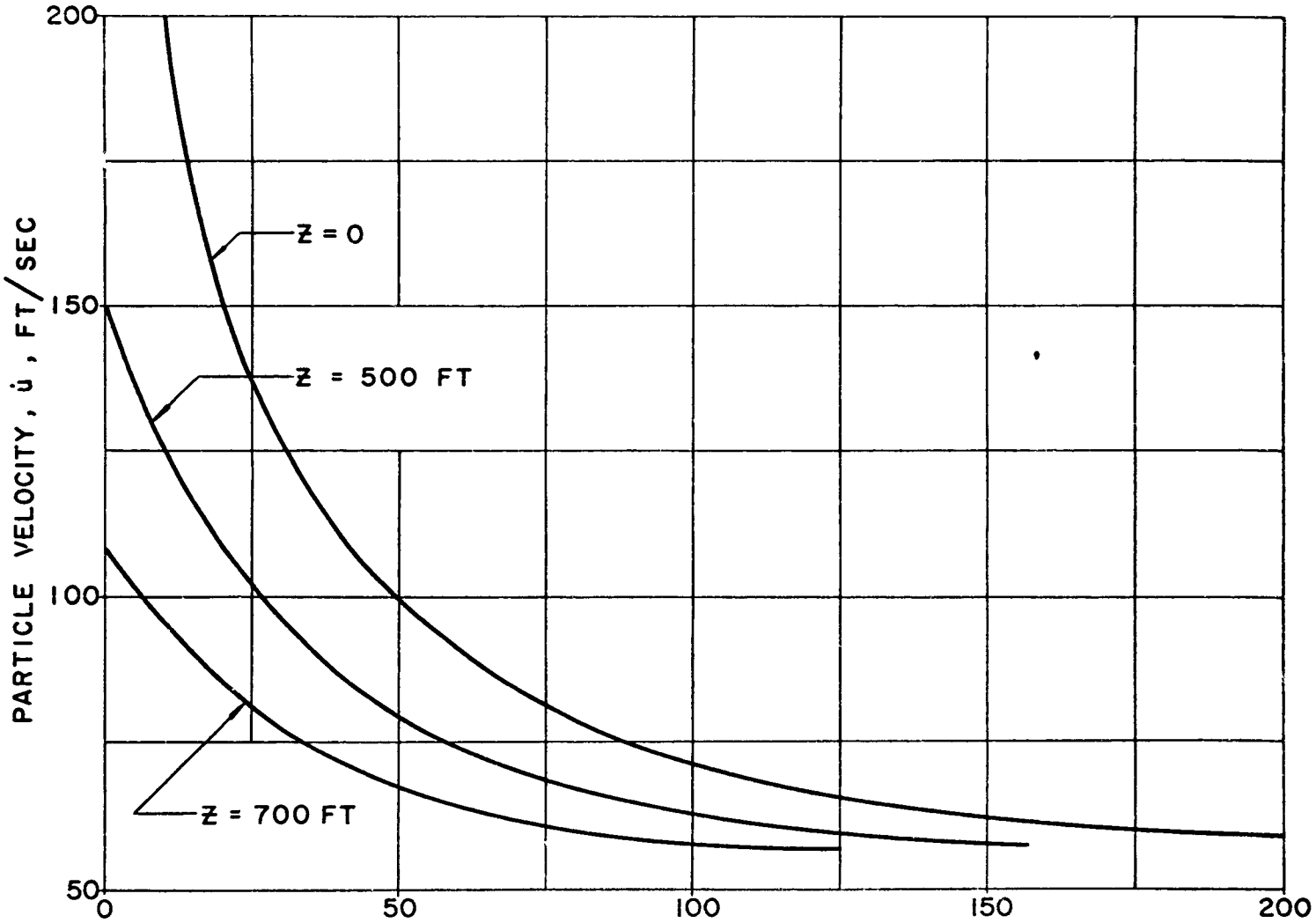

FIG. 9 PARTICLE VELOCITIES IN PLASTIC-ELASTIC MEDIUM

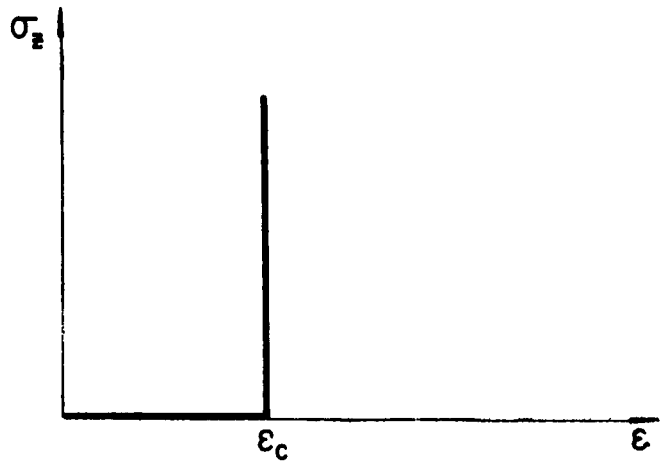

FIG. 10 STRESS–STRAIN DIAGRAM OF LOCKING MEDIUM

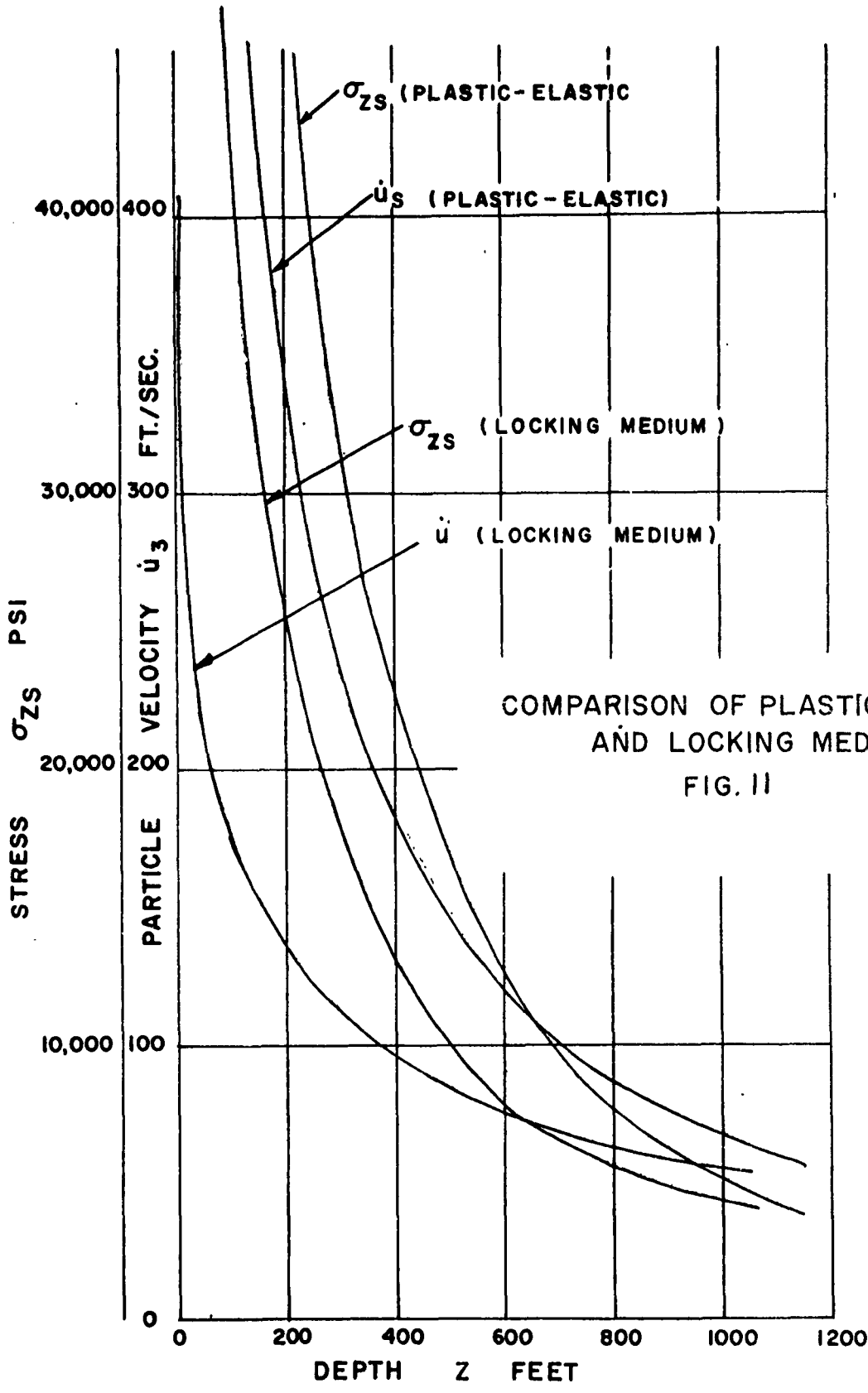

COMPARISON OF PLASTIC-ELASTIC AND LOCKING MEDIA

FIG. 11

SECTION III

SPHERICAL WAVES IN AN IDEAL LOCKING MEDIUM

by

Mario G. Salvadori[1]
Richard Skalak[2]
Paul Weidlinger[3]

(1) Professor of Civil Engineer, Columbia University, and Associate, Paul Weidlinger, Consulting Engineer, New York, New York.

(2) Associate Professor of Civil Engineering, Columbia University, New York, New York

(3) Consulting Engineer, New York, New York

SYNOPSIS

Asymptotic short time and long time solutions are derived in closed form for the spherical wave propagation in an infinite, ideal locking medium due to various types of time varying pressures applied to the surface of a spherical cavity. Among these are: (a) a constant pressure; (b) a center of dilatation; (c) an adiabatic gas expansion; (d) an energy input due to an exploding point mass.

INTRODUCTION

The propagation of plane waves in various types of locking media has been considered by several authors [4], [5], [6]. Spherical waves in plastic locking media were investigated by Kompaneets [7] and more recently by Zvolinskii who derived the wave equations for an elasto-plastic medium of limited compressibility [8].

Since, in general, closed form solutions of this type of problem cannot be obtained, asymptotic closed form solutions are given in this paper for an infinite ideal locking medium. An equation of motion is first derived for large strains and displacements when a variable pressure is applied to the surface of a spherical cavity. It is then shown that its

---

[4] "Stress Waves in Dissipative Media" by M. G. Salvadori, R. Skalak, P. Weidlinger, Transactions New York Academy of Science, Ser. II, Vol. 21, No. 5, pp 427-434, 1959.

[5] " Waves and Shocks in Locking and Dissipative Media" by M. G. Salvadori, R. Skalak, P. Weidlinger, Journal Engineering Mechanics Division, ASCE, Vol.86, April 1960

[6] "On the Plane Motion of Sand" by A. I. Ishlinskii, Ukr.Math. Journal, Vol. 6, No. 4, 1954.

[7] "Shock Waves in Plastic Compacting Media" by A. S. Kompaneets, Proc. Academy of Science , USSR, 1956, Vol. 106, No. 1, pp 49-52.

[8] " "On the Emission of an Elastic Wave from a Spherical Explosion in the Ground" by N. V. Zvolinskii, P. M. M. Vol. 24, No. 1, 1960, pp 126-133.

early time asymptotic solution is the rigorous solution of the same problem when small strains and displacements are considered. The long time asymptotic solution of the same equation is then shown to be the rigorous solution for a point source pressure when large strains and displacements are again considered.

The behavior of a three-dimensional ideal locking medium under compressive stresses is characterized as follows:

(a) At first the material of initial density ρ_o does not offer resistance to compression but, once a critical value of the strain is reached, the density changes abruptly to a value ρ_1 and a constant value of the dilatation:

$$\ell = 1 - \rho_o/\rho_1 < 1 \qquad (1)$$

is maintained from then on (Figure 1) .

(b) During the subsequent motion with a constant density ρ_1 the material satisfies the three-dimensional yield condition derivable from Coulomb's law of failure [9] :

$$\sigma_r - \sigma_\theta = -c + \frac{1 - k}{1 + k} (\sigma_r + \sigma_\theta) \qquad (2)$$

where, due to symmetry, the radial and tangential stresses σ_r, σ_θ are principal stresses, the constant c is proportional to the cohesion, and k is a function of the coefficient of internal friction.

The above described behavior is typical of certain cohesive granular soils under high compressive stresses. Since under such stresses the effect of cohesion becomes negligible as compared to that of friction,

---

[9] "On Coulomb's Law of Failure in Soils", by R. T. Shield, Journal Mech. Phys. Solids, 4(1955), pp 10-16, May 1960.

Equation (2) becomes:

$$\sigma_\theta = k\sigma_r \tag{3}$$

with

$$0 \leq k \leq 1 \tag{3a}$$

2. SPHERICAL WAVE EQUATIONS.

Consider a spherical cavity of initial radius r_i in an infinite ideal locking medium. From t = 0 on the cavity boundary is subjected to a uniform pressure of intensity p, which is a function of the expanding cavity radius r_o. Let r be the Lagrangian coordinate of a particle, and w its radial displacement at a time t, when the medium has been compacted to a density ρ_1 up to a distance R from the cavity center, while beyond R the medium is at rest with a density ρ_o (Figure 2).

Under these assumptions conservation of mass requires that:

$$(r - w)^3 = \frac{1}{1 - \xi} r^3 - \frac{\xi}{1 - \xi} R^3 \tag{4}$$

and, in particular, that at the cavity boundary, where $r = r_i + w_o = r_o$:

$$x = \frac{R}{r_o} = \left[\xi + (1 - \xi)(r_i/R)^3 \right]^{-1/3} \tag{5}$$

For $\xi \ll 1$, and at an early time when the change in the cavity radius is negligible, so that $r_o \approx r_i$, the ratio x approaches the value:

$$x_s = R/r_i \tag{6}$$

At late times when R is large enough for $(1 - \xi)(r_i/R)^3$ to be much less than ξ, the ratio x approaches the constant value:

$$x_L = \xi^{-1/3} \tag{7}$$

Denoting time derivatives by dots, the particle velocity at r ($\dot{w} = \dot{r}$) becomes, by Equation (4):

$$\dot{w} = (R/r)^2 \xi\dot{R} \tag{8}$$

and at the wave front (r = R):

$$\dot{w}\Big]_{r = R} = \xi\dot{R} \tag{9}$$

The particle acceleration, by Equation (8), becomes:

$$\ddot{w} = \xi(R^2\ddot{R} + 2R\dot{R}^2)r^{-2} - 2\xi^2R^4\dot{R}^2r^{-5} \tag{10}$$

The equation of motion for an elementary volume of soil in spherical coordinates (Figure 3) is given by:

$$\frac{\partial\sigma_r}{\partial r} + \frac{2(1 - k)}{r}\,\sigma_r = -\rho_1\ddot{w} \tag{11}$$

where $\ddot{w}$ is defined by Equation (10), and its particular solution satisfying the boundary condition:

$$\sigma_r\Big]_{r = r_o} = p(r_o) \tag{12}$$

is for $k \neq 1/2$:

$$\sigma_r = p(r_o)\left(\frac{r}{r_o}\right)^{-2+2k} + \frac{\rho_1\xi}{(1 - 2k)r_o}(R^2\ddot{R} + 2R\dot{R}^2)\left[\left(\frac{r}{r_o}\right)^{-2+2k} - \left(\frac{r}{r_o}\right)^{-1}\right] + \frac{\rho_1\xi^2}{(1 + k)r_o^4}R^4\dot{R}^2\left[\left(\frac{r}{r_o}\right)^{-2+2k} - \left(\frac{r}{r_o}\right)^{-4}\right] \tag{13}$$

and for $k = 1/2$:

$$\sigma_r = p(r_o)\left(\frac{r}{r_o}\right)^{-1} - \frac{\rho_1\xi}{r_o}(R^2\ddot{R} + 2R\dot{R}^2)\left(\frac{r}{r_o}\right)^{-1}\ell n\left(\frac{r}{r_o}\right) + \frac{2}{3}\frac{\rho_1\xi^2}{r_o^4}R^4\dot{R}^2\left[\left(\frac{r}{r_o}\right)^{-1} - \left(\frac{r}{r_o}\right)^{-4}\right] \qquad (k = 1/2) \tag{13a}$$

Conservation of momentum across the wave front (r = R) requires, by Equation (9), that:

$$\sigma_r\Big]_{r=R} = \rho_1 \xi(1-\xi)\dot{R}^2 \qquad (14)$$

Setting this value of σ_r in Eq.(13),(13a), and making use of Equation (5), the equation governing the motion of the wave front becomes:

$$\alpha R \frac{d\dot{R}^2}{dR} + \beta \dot{R}^2 = \frac{2p}{\rho_1 \xi(1-\xi)} \qquad (15)$$

in which the variable coefficients α and β are given for $k \neq 1/2$ by:

$$\alpha = \frac{1}{(2k-1)(1-\xi)} \left(x - x^{2-2k}\right)$$

$$\beta = 2\left[x^{2-2k} + \frac{2}{(2k-1)(1-\xi)}\left(x - x^{2-2k}\right) - \frac{2}{(1+k)(1-\xi)}\left(x^4 - x^{2-2k}\right)\right] \qquad (k \neq 1/2) \qquad (16)$$

and for $k = 1/2$ by:

$$\alpha = \frac{1}{1-\xi} \, x \ell n \, x$$

$$\beta = 2\left[x + \frac{2}{1-\xi} \, x \ell n \, x - \frac{2}{3}\frac{\xi}{1-\xi}\left(x^4 - x\right)\right] \qquad (k = 1/2) \qquad (16a)$$

III. Short Time Asymptotic Solution (Finite cavity, small strain, small displacement solution).

Substituting $x = x_s$ from Equation (6) into Equations (16) one obtains the differential equation valid for small displacements. A further simplification is obtained by considering the strains to be small, i.e., neglecting terms in ξ^2 and, hence, the third term at the right hand member of β in

Equations (16) or (16a). Since Equation (6) is valid when the expansion of the cavity is negligible, and the pressure p is considered a function of the cavity radius r_o, the pressure is to be assumed constant:

$$p(r_o) = p_o \tag{17}$$

For an explosion of yield W and gas constant γ:

$$p_o = (\gamma - 1)\frac{W}{4/3\pi r_1^3} \quad [10] \tag{a}$$

The solution of Equation (15) in terms of the non-dimensional wave front radius:

$$x_s = R/r_1 \tag{6a}$$

thus becomes:

$$\dot{x}_s^2 = \frac{2(2k-1)p_o}{\rho_1 \xi r_1^2} \frac{1}{x_s^4(1 - x_s^{1-2k})^2}\left[\frac{1}{3}(x_s^3 - 1) - \frac{1}{4-2k}(x_s^{4-2k} - 1)\right] \tag{18}$$

The corresponding solution for k = 1/2 is:

$$\dot{x}_s^2 = \frac{2}{9}\frac{p_o}{\rho_1 \xi r_1^2} \frac{1}{x_s^4 \ell n^2 x_s}\left[x_s^3(3\ell n\, x_s - 1) + 1\right] \tag{18a}$$

IV. Long Time Asymptotic Solution (Point Source, finite strain, large displacement solution).

Assuming for x the value $\xi^{-1/3}$ given by Equation (7), the coefficients α and β of Equation (15) become constant, and depend on ξ and k only. This equation, rigorously valid for $r_1 = 0$, coincides with the equation derived by Kompaneets.[7]

[10] "A Method of Concealing Underground Nuclear Explosions" by A. L. Latter, R. E. LeDevier, E. A. Martinelli, W. G. McMillan; R-348, The RAND Corporation, March 30, 1959.

The following particular solutions of this equation are of interest:

(a) Center of Dilatation.

The magnitude P_o of the total force exerted on the cavity surface is constant in time so that, letting:

$$P_o = \lim_{r_1 \to 0} 4\pi\rho(r_1)r_1^2 \qquad (19)$$

the variable pressure p, by Equations (4) and (9), becomes:

$$p(R) = \frac{P_o}{4\pi t^{2/3}} R^{-2} \qquad (20)$$

The corresponding solution of Equation (15) is:

$$\dot{R}^2 = \frac{P_o}{\rho_1 t} \frac{1}{2\pi t^{2/3}(\beta - 2\alpha)(1 - \xi)} R^{-2} \qquad (21)$$

If at a time $t = t_1$, when $R = R_1$, P_o becomes zero, the wave front propagates with a velocity:

$$\dot{R}^2 = \frac{P_o}{\rho_1 t} \frac{R_1^{-2}}{2\pi t^{2/3}(\beta - 2\alpha)(1 - \xi)} \left(\frac{R}{R_1}\right)^{-\beta/\alpha} \quad (R \geq R_1) \qquad (22)$$

Since $\beta/\alpha > 2$ for all values of ξ and k, $\dot{R}^2$ approaches zero asymptotically and the wave front never stops. This result stems from the neglection of the cohesion c in Equation (2): a finite value of c gives a finite time at which the motion stops.

(b) Expansion of An Ideal Gas.

In the expansion of an ideal gas the pressure p follows the law:

$$\lim_{r_1 \to 0} p(r_1)r_1^{3\gamma} = p(r_o)r_o^{3\gamma} = K \qquad (23)$$

where γ and K are constant characteristics of the gas and of the energy of the explosion.

The solution of Equation (15) when the pressure $p(r_o)$ is defined by Equation (23) and $\beta/\alpha > 3\gamma$ [11], is:

$$\dot{R}^2 = \frac{2K}{\rho_1 \xi} \frac{\xi^{-\gamma}}{(\beta - 3\alpha\gamma)(1-\xi)} R^{-3\gamma} \tag{24}$$

In this case also the introduction of a finite value for the cohesion introduces a finite stopping time, as shown by Kompaneets [7]

(c) Exploding point mass. [12]

Consider a point mass M located in the medium at r = 0, which at t = 0 explodes so that its particles acquire a radial velocity $\dot{r}_o$. Assuming that these particles remain on the boundary surface of an expanding spherical cavity of radius r_o, the total kinetic energy at a time t is:

$$T = \frac{1}{2} \int_{r_o}^{R} 4\pi\rho_1 r^2 \dot{r}^2 \, dr + \frac{1}{2} M \dot{r}_o^2 \tag{25}$$

and, by Equations (7), (8) and (25), the rate of increase of this energy is:

$$\frac{dT}{dR} = \left[4\pi\rho_1 (\xi^{-1/3} - 1) R^3 + M\xi^{-4/3} \right] \xi^2 \dot{R} \frac{d\dot{R}}{dR} + 6\pi\rho_1 \xi^2 (\xi^{-1/3} - 1) R^2 \dot{R}^2 \tag{26}$$

The rate of energy loss across the shock front is (Figure 4):

$$\frac{dE}{dR} = -\frac{1}{2} \sigma_x \Big]_{r=R} \xi \tag{27}$$

In the particular case of k = 1 no other energy loss can occur within the medium so that:

$$\frac{dT}{dR} + \frac{dE}{dR} = 0 \tag{28}$$

Hence by Equations (26) and (27):

$$(R^3 + r_m^3) \frac{d\dot{R}}{dR} + 3\mu R^2 \dot{R} = 0 \tag{29}$$

---

(11) For $\beta/\alpha < 3\gamma$ there are no solutions of the point source equation.

[12] The authors are indebted to Dr. H. H. Bleich for this solution.

where

$$r_m^3 = \frac{M}{4\pi\rho_1(\xi^{-1} - \xi^{-2/3})\xi^2} \qquad \mu = \frac{1}{2} + \frac{1-\xi}{6(\xi^{-1/3} - 1)} \qquad (30)$$

The solution of Equation (29) with $\dot{R}(0) = \dot{R}_o$, and hence an energy input $\frac{1}{2} M \dot{R}_o^2$, is

$$\frac{\dot{R}}{\dot{R}_o} = \left[1 + \left(\frac{R}{r_m}\right)^3\right]^{-\mu}$$

where $1/2 < \mu < 1$ for $0 < \xi < 1$.

VI. Intermediate Range Solutions.

The variable coefficients α and β of Equation (15) approach their asymptotic values for $R \longrightarrow \infty$, but become practically constant at finite values of R depending on k and ξ. For example, the behavior of α and β versus $x_s = R/r_i$ is given in Figures (5a) and (5b) for $k = 1, 1/2$, and 0 when $\xi = 0.1$.

The solution of Equation (15) in the intermediate range between the two asymptotic short time and long time solutions may be obtained by numerical means starting at the limit of the range of validity for either solution and integrating forward or backward, respectively.

The constant K, needed to continue the intermediate time solution for an explosion is obtained by Equation (23). Table I shows the range of validity of the two asymptotic solutions.

Table I

($\xi = 0.1$)

	Short Time								Long Time		
$\frac{R}{r_i}$	1.00	1.02	1.04	1.06	1.08	1.10	1.25	1.50	10	20	∞
x_s	1.00	1.02	1.04	1.06	1.08	1.10	1.25	1.50	--	--	--
x	1.00	1.02	1.04	1.05	1.07	1.09	1.21	1.40	2.14	2.15	2.15
x_L	--	--	--	--	--	--	--	--	2.15	2.15	2.15

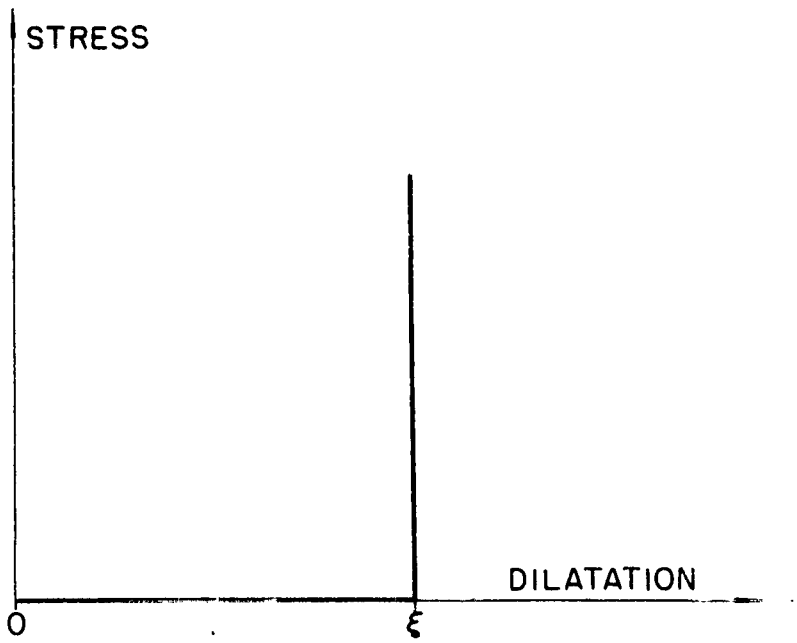

FIG. 1

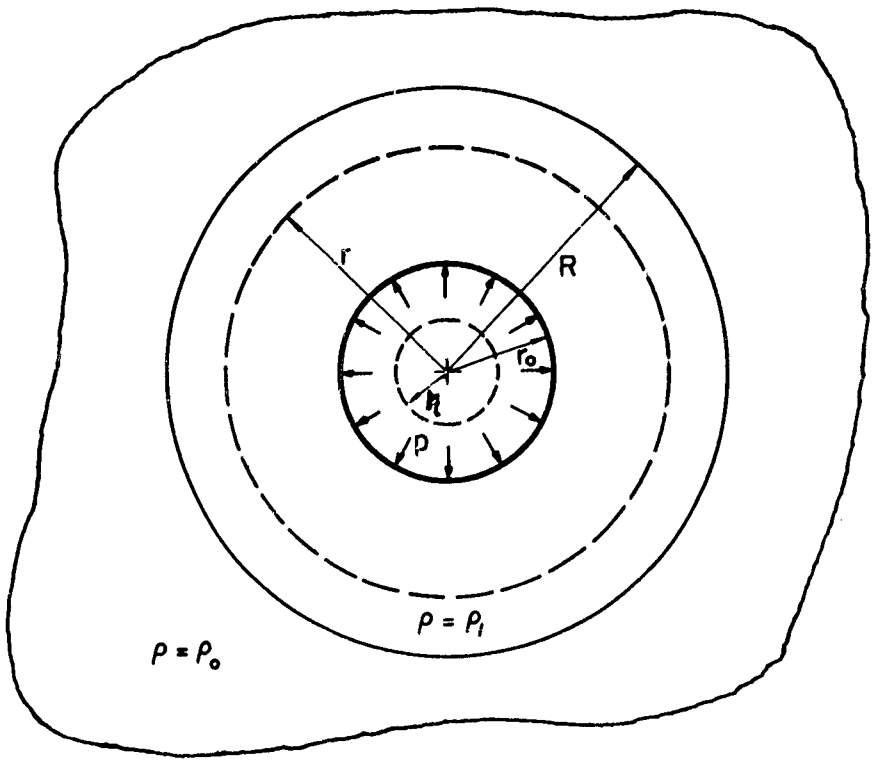

FIG. 2

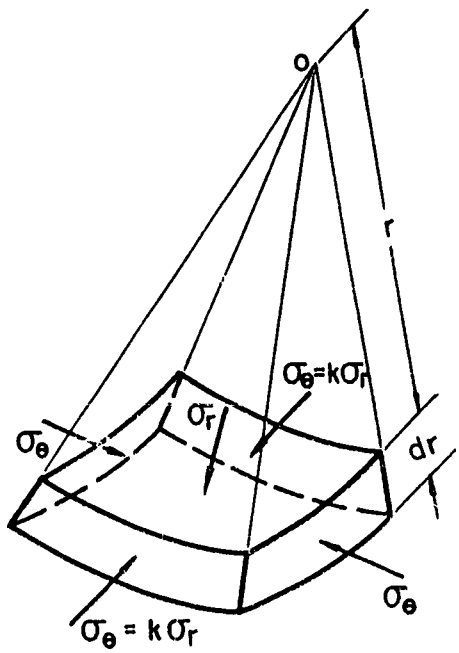
o
r
$\sigma_\theta = k\sigma_r$
σ_r
σ_θ
dr
σ_θ
$\sigma_\theta = k\sigma_r$

FIG. 3

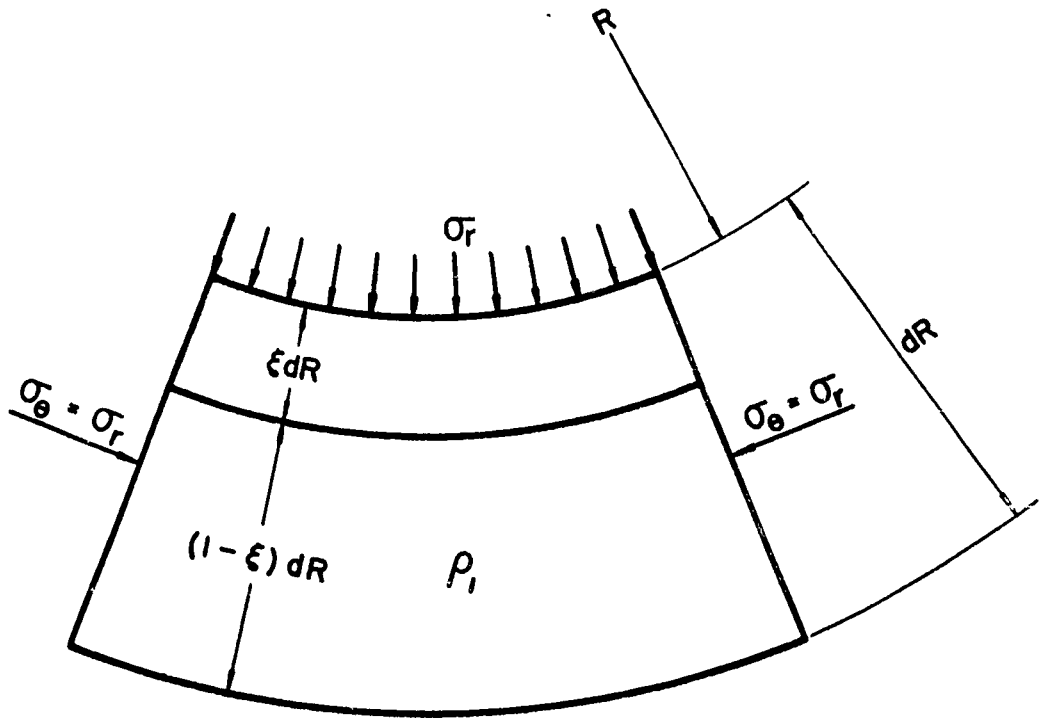
R
σ_r
ξdR
$\sigma_\theta = \sigma_r$
$\sigma_\theta = \sigma_r$
dR
$(1-\xi)\,dR$
ρ_1

FIG. 4

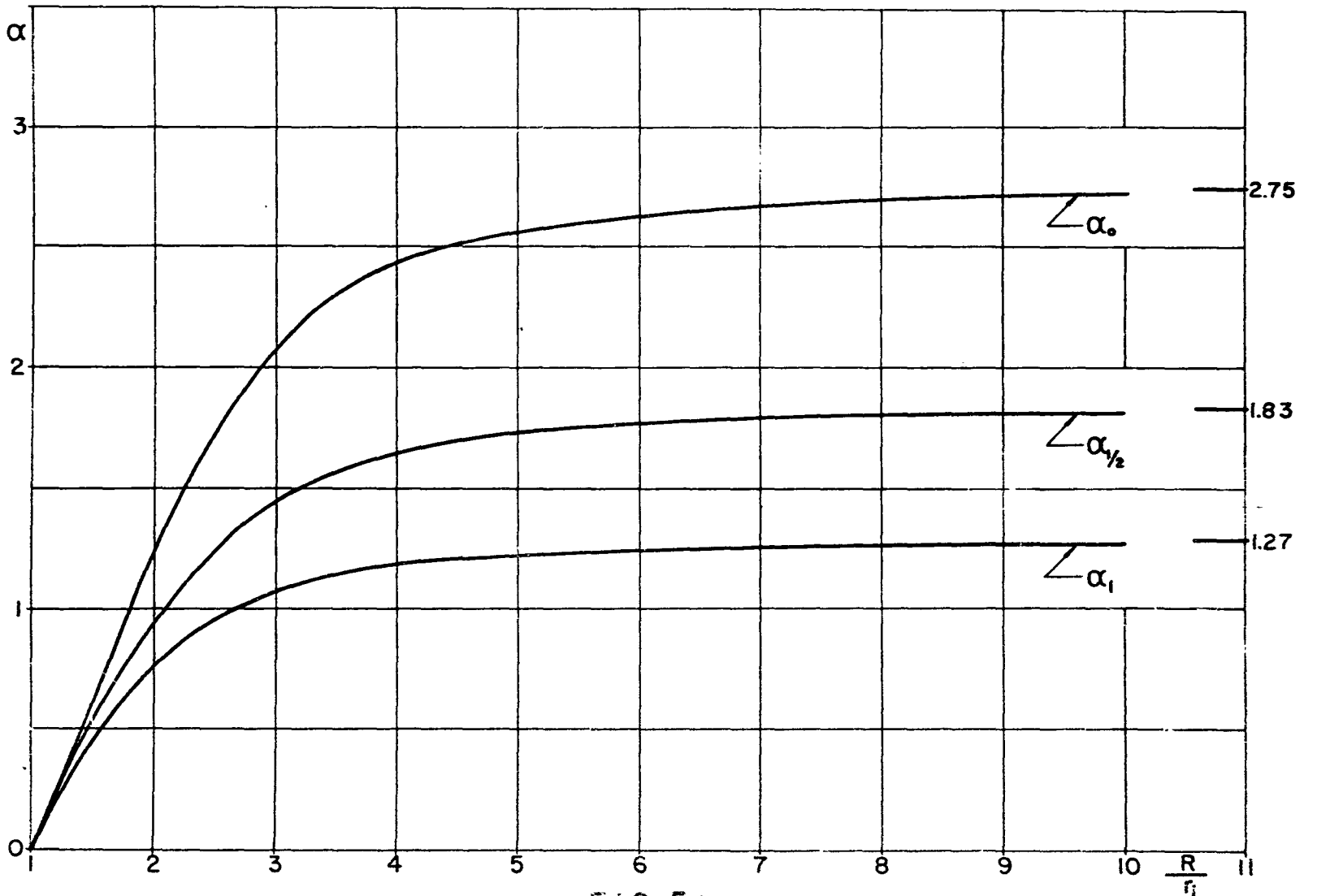

FIG. 5a

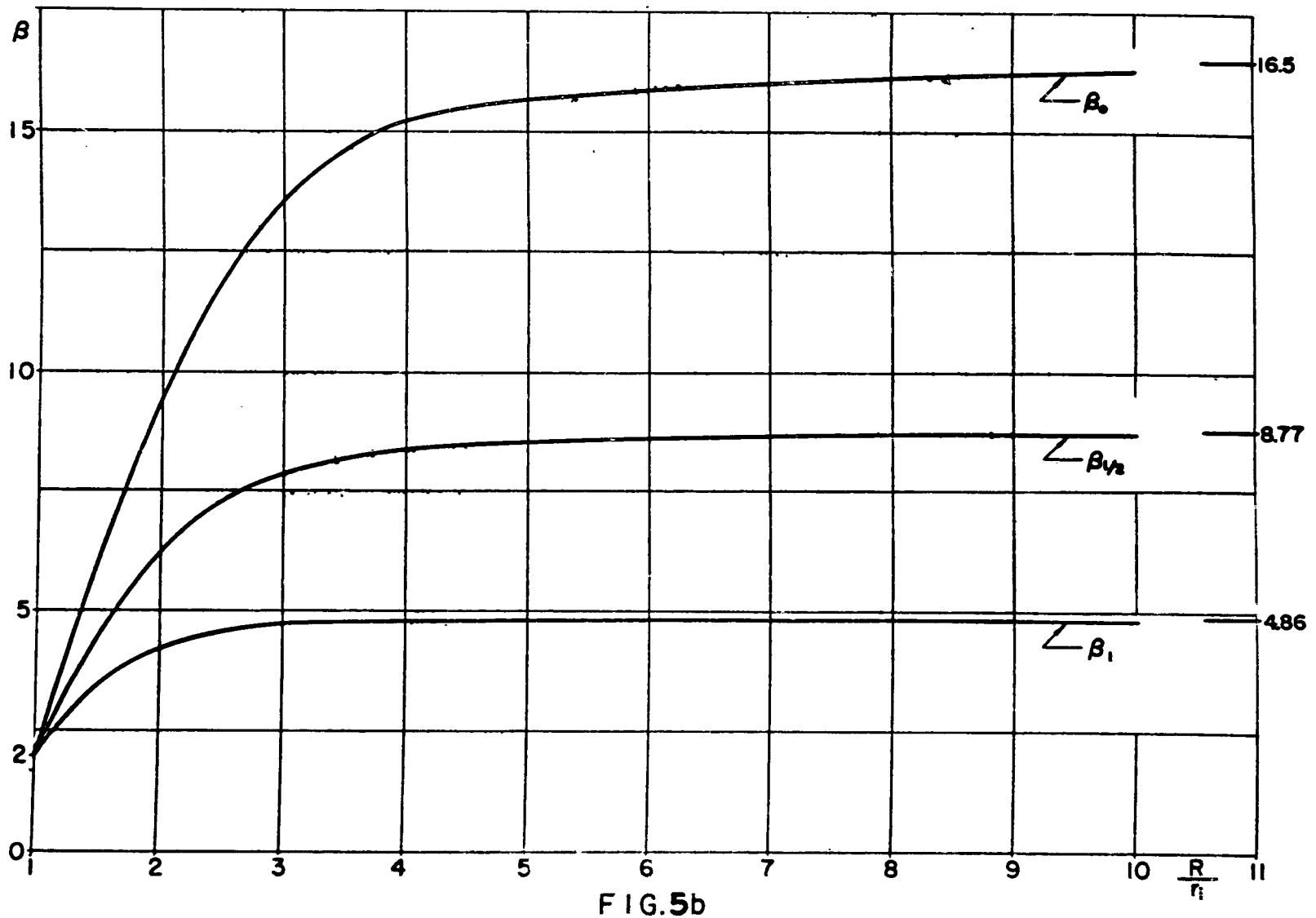

FIG.5b